

Entry flow in heated curved pipes

N. PADMANABHAN

Centre for Atmospheric Sciences, Indian Institute of Technology,
Hauz Khas, New Delhi 110016, India

(Received 10 February 1986)

Abstract—The flow in the entrance region of heated curved pipes is analysed. Two cases of heating—a constant temperature at the wall, and a constant flux of heat at the wall—are considered. Using boundary layer approximations and the method of matched asymptotic expansions, the combined effects of curvature, entrance region and the buoyancy is studied. It is found that buoyancy disturbs the symmetric secondary motion induced by curvature, the deviation depending on the type of thermal input at the wall. It is also found that the oscillatory nature of the Nusselt number in the constant temperature case decreases as the Peclet number is increased.

INTRODUCTION

THE STUDY of developing flow has attracted much attention in the last decade, in view of its possible implications in blood flows in the cardiovascular system and in other engineering problems. The entry regions in the arteries have been identified as the regions most prone to the development of atherosclerosis—a disease manifested by the thickening of the arterial wall. In engineering applications, it has been found experimentally, that the pumping power needed to maintain a given flux in the developing region is more than that needed in the fully developed region. Besides the experimental studies, numerous theoretical analyses have been undertaken to give a proper mathematical model for the flow in the developing region.

The introduction of thermal boundary conditions at the wall of a pipe affects the flow quite drastically. Depending on the relative magnitudes of buoyancy and viscous forces, either a free convection or a forced convection is set up. In either case, a secondary flow is set up even in a straight pipe. Morton [1] showed the development of secondary flow for small $Re Ra$, where Re is the Reynolds number and Ra the Rayleigh number—the product giving a measure of the ratio of buoyancy forces to viscous forces. Mori and Nakayama [2] extended the analysis to higher values of $Re Ra$. With physiological applications in mind, Mahalakshmi and Devanathan [3] obtained the solution for heat transfer in tubes of varying cross-sections.

In this paper, we study the entry flow in a heated curved pipe. The first theoretical analysis of flow in curved pipes was given by Dean [4, 5]. He showed that the flow depended on a single non-dimensional parameter $D = (2\delta)^{1/2} Re$, now called the Dean number. Since the solution was obtained as a regular perturbation on D , the analysis was restricted to $D < 96$. Since then, various authors have tried to relax this restriction on D . McConologue and Srivastava

[6], using numerical methods obtained accurate results for $D < 600$, while Collins and Dennis [7] went up to $D \approx 5000$. Barua [8] using the method of matched asymptotic expansions established the existence of a boundary layer on the inside of a curved pipe.

The problem of entry flow in heated straight pipes has been looked into by various authors. Lawrence and Chato [9] developed a numerical method for the calculation of entrance flows in vertical tubes. They found that the transition to turbulence depended on the initial velocity profiles and the thermal condition on the wall. Yao [10] obtained the solution to the problem as a perturbation of the developing flow in an unheated straight pipe, and observed two secondary vortices resulting from the combination of radial directional motion and the vertical downward motion.

This paper deals with the entry flow in a heated curved pipe. We consider two different kinds of heating at the wall—a constant temperature T_w , and a constant flux of heat at the wall, q_w , herein after referred to as cases I and II, respectively. Singh [11] considered the entry flow in an unheated curved pipe, and obtained the solution as a perturbation on the straight tube solution for small values of δ , the curvature parameter, while Yao and Berger [12] obtained a numerical solution to the same problem. Pedley [13] using a different set of scales to incorporate the curvature effect overcame this restriction on δ . An excellent review of entry flow in pipes, heated, unheated, straight or curved is given in Yao [10], and Yao and Berger [14].

FORMULATION OF THE PROBLEM

We assume that the fluid enters the pipe from a reservoir of constant pressure head, with a constant temperature T_0 . The wall is assumed to be kept at constant temperature T_w in case I, while in case II, it is assumed that there is a constant flux of heat q_w

NOMENCLATURE

a	radius of cross-section of the pipe	(R, ϕ, α)	coordinates of any point in the toroidal system
b	radius of curvature of the pipe	(U, V, W)	velocity of the fluid
D	Dean's number	(u, v, w)	non-dimensional velocity of the fluid
Gr	Grashof number	(u_1, v_1, w_1)	velocity in the boundary layer.
k	conductivity of the fluid	Greek symbols	
\bar{p}	non-dimensional pressure	δ	curvature ratio, a/b
\bar{P}	dimensional pressure	ε	Gr/Re^2 in case I, and $Gr/Re^{5/2}$ in case II
Pr	Prandtl number	η	boundary layer coordinate in the radial direction
q_w	constant flux of heat at the wall—case II	θ	non-dimensional temperature
Re	Reynolds number	ρ	density.
T_0	constant inlet temperature		
T_w	constant temperature at the wall		
W_0	constant entry velocity		

at the wall. Figure 1 shows the toroidal system of coordinates used. The pipe is supposed to be coiled in the form of a circle with centre 0, radius b and $0Z$ as the axis. The centre of the cross-section of the pipe C is in a plane making an angle α with a fixed axial plane. The length of $0C$ is b , the radius of curvature of the pipe. The plane passing through 0 and perpendicular to $0Z$ is called the central plane, and the circle traced out by C is the central line. Any point P in the flow field is identified by its coordinates (R, ϕ, α) , where R is the distance CP , ϕ is the angle made by CP with $0C$ extended. Let the velocity components in this coordinate system be (U, V, W) .

We first consider case I, where the fluid enters the tube from a constant dynamic pressure head at a temperature T_0 , and the wall is kept at a constant temperature T_w . Thus, the entry conditions are

$$\begin{aligned}
 U &= 0 \\
 V &= 0 \\
 W &= bW_0/(b + R \cos \phi) \\
 T &= T_0.
 \end{aligned}
 \tag{1}$$

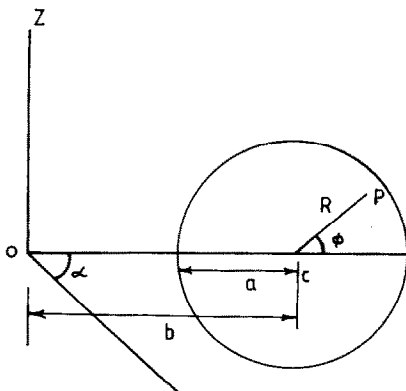


FIG. 1. Coordinate system.

The variables are non-dimensionalized as follows:

$$\begin{aligned}
 (u, v, w) &= (U, V, W)/W_0, & \bar{p} &= \bar{P}/\rho W_0^2 \\
 \theta &= (T - T_w)/(T_w - T_0), & r &= R/a
 \end{aligned}
 \tag{2}$$

where a is the radius of the pipe.

Writing $s' = b\alpha$, and $s = s'/a$, the governing equations are

$$u_r + \frac{1 + 2\delta r \cos \phi}{hr} u + \frac{v_\phi}{r} - \frac{v\delta \sin \phi}{h} + \frac{w_s}{h} = 0
 \tag{3}$$

$$\begin{aligned}
 uu_r + \frac{vu_\phi}{r} + \frac{wu_s}{h} - \frac{v^2}{r} - \frac{\delta \cos \phi}{h} w^2 &= -\bar{p}_r \\
 &+ \frac{Re^{-1}}{rh} \left\{ \frac{\partial}{\partial s} \left[\frac{r}{h} (u_s - hw_r - \delta \cos \phi w) \right] \right. \\
 &\left. - \frac{\partial}{\partial \phi} \left[h \left(v_r + \frac{v}{r} - \frac{u_\phi}{r} \right) \right] \right\} + \varepsilon \theta \sin \phi
 \end{aligned}
 \tag{4}$$

$$\begin{aligned}
 uw_r + \frac{vw_\phi}{r} + \frac{ww_s}{h} + \frac{uw}{r} + \frac{\delta \sin \phi}{h} w^2 &= -\frac{\bar{p}_\phi}{r} \\
 &+ \frac{Re^{-1}}{h} \left\{ \frac{\partial}{\partial r} \left[h \left(v_r + \frac{v}{r} - \frac{u_\phi}{r} \right) \right] \right. \\
 &\left. - \frac{\partial}{\partial s} \left[\frac{1}{rh} (hw_\phi - \delta r \sin \phi w - ru_s) \right] \right\} + \varepsilon \theta \cos \phi
 \end{aligned}
 \tag{5}$$

$$\begin{aligned}
 uw_r + \frac{vw_\phi}{r} + \frac{ww_s}{h} + \frac{\delta \cos \phi}{h} uw - \frac{\delta \sin \phi}{h} vw \\
 = -\frac{\bar{p}_s}{h} + \frac{Re^{-1}}{r} \left\{ \frac{\partial}{\partial \phi} \left[\frac{1}{rh} (hw_\phi - \delta r \sin \phi w - ru_s) \right] \right. \\
 \left. - \frac{\partial}{\partial r} \left[\frac{r}{h} (u_s - hw_r - \delta \cos \phi w) \right] \right\}
 \end{aligned}
 \tag{6}$$

$$\begin{aligned}
 u\theta_r + \frac{v\theta_\phi}{r} + \frac{w\theta_s}{h} &= \frac{1}{Pr Re} \left[\theta_{rr} + \frac{\theta_r}{r} \right. \\
 &\left. + \frac{\delta \cos \phi}{h} \theta + \frac{\theta_{\phi\phi}}{r^2} - \frac{\delta \sin \phi}{rh} \theta_\phi + \frac{\theta_{ss}}{h^2} \right]
 \end{aligned}
 \tag{7}$$

where

$$h = 1 + \delta r \cos \phi$$

$$\delta = a/b$$

$$Re = \text{Reynolds number} = W_0 a / \nu$$

$$Pr = \text{Prandtl number} = \nu/k$$

$$\varepsilon = Gr/Re^2, \text{ where } Gr \text{ is the Grashof number.}$$

The corresponding boundary conditions are

$$u = v = 0, \quad w = 1/h, \quad \theta = -1 \quad \text{at } s = 0$$

and (8)

$$u = v = w = \theta = 0 \quad \text{on } r = 1.$$

In writing down these equations of motion, we have invoked the Boussinesq approximation by assuming that the density variations due to heating occurs only in the buoyancy terms. This approximation is valid when the fluid density changes only by a small amount.

SOLUTION

As the fluid enters the pipe, viscous forces are confined to the wall of the pipe. Thus, the flow field can be divided into two regions—a boundary layer, in which the viscous forces are balanced by the inertia forces, and a core region, in which the centrifugal forces arising out of the curvature of the pipe is balanced by the pressure gradient. Apart from these forces, heating of the wall gives rise to buoyancy forces inside the thermal boundary layer. The ratio of the thermal boundary layer thickness to momentum boundary layer thickness depends on Prandtl number. In the core region, the effects of both viscosity and heat conduction can be ignored. The equations in the core region can be obtained from equations (3)–(7) by letting $Re \rightarrow \infty$. The solutions to these reduced equations are

$$u^c = v^c = 0, \quad w^c = 1/h, \quad \bar{p}^c = -1/2h^2, \quad \theta^c = -1. \tag{9}$$

For solutions in the boundary layer, we observe that near the entrance, the flow will be similar to that past a flat plate. Keeping this in mind, we rescale the variables as follows:

$$\eta = \frac{Re^{1/2}(1-r)}{h_0\sqrt{(2s)}}, \quad u = \frac{Re^{-1/2}u_1}{h_0\sqrt{(2s)}},$$

$$v = v_1, \quad w = \frac{w_1}{h_0} \tag{10}$$

where

$$h_0 = 1 + \delta \cos \phi.$$

Equations (3)–(7) are then transformed into

$$\eta v_{1\eta} + \eta w_{1\eta} - 2sw_{1s} \left[v_{1\phi} + \frac{\delta \sin \phi}{h_0} (\eta v_{1\eta} - v_1) \right] \tag{11}$$

$$\bar{p}_\eta = 0 \quad \text{provided } Gr \ll Re^{5/2} \tag{12}$$

$$v_{1\eta\eta} + u_1 v_{1\eta} + w_1 (\eta v_{1\eta} - 2sw_{1s}) - 2sh_0^2 \bar{p}_\phi$$

$$= 2sh_0^2 \left[v_1 \left(v_{1\phi} + \frac{\delta \sin \phi}{h_0} \eta v_{1\eta} \right) + \frac{\delta \sin \phi}{h_0^3} w_1^2 - \varepsilon \theta \cos \phi \right] \tag{13}$$

$$w_{1\eta\eta} + u_1 w_{1\eta} + w_1 (\eta w_{1\eta} - 2sw_{1s}) - 2sh_0^2 \bar{p}_s$$

$$= 2sh_0^2 \left[v_1 \left(w_{1\phi} + \frac{\eta w_{1\eta} \delta \sin \phi}{h_0} \right) \right] \tag{14}$$

$$\theta_{\eta\eta} + u_1 \theta_\eta + w_1 (\eta \theta_\eta - 2s\theta_s)$$

$$= 2sh_0^2 v_1 \left[\theta_\phi + \frac{\eta \theta_\eta \delta \sin \phi}{h_0} \right] \tag{15}$$

with boundary conditions

$$u_1 = v_1 = w_1 = \theta = 0 \quad \text{on } \eta = 0$$

$$u_1, w_1, \theta \rightarrow u^c, w^c, \theta^c \quad \text{as } \eta \rightarrow \infty.$$

The scaling in equation (10) has been done in such a way that near the entrance, the flow is similar to that on a flat plate. Accordingly, we expand all variables in powers of s . Thus

$$R_i = \sum_{n=0}^{\infty} s^n R_{in}(\eta, \phi) \tag{16}$$

where R stands for u, v, w and θ . Using these expansions in the boundary layer equations (11)–(15) and solving the various order terms, we obtain the following expressions for the velocity components and temperature in the boundary layer:

$$u = (f_0 - \eta f'_0) + s^2 [4h_0 \delta \cos \phi - 4\delta^2 \sin^2 \phi] (f_1 + 5F_1 - \eta F'_1)$$

$$- (16h_0^3 \delta \varepsilon \sin \phi \cos \phi + 4h_0^4 \varepsilon \sin \phi) (f_2 + 5F_2 - \eta F'_2) + 4\delta^2 \sin^2 \phi f'_1 + 4\varepsilon \delta h_0^3 \sin \phi \cos \phi f'_2 \tag{17}$$

$$v = s \left[\frac{2\delta \sin \phi}{h_0} f'_1 + 2h_0^2 \varepsilon \cos \phi f'_2 \right] \tag{18}$$

$$w = f'_0 + s^2 [4\delta (h_0 \cos \phi - \delta \sin^2 \phi) F'_1 - (4h_0^4 \varepsilon \sin \phi + 16h_0^3 \varepsilon \delta \sin \phi \cos \phi) F'_2] \tag{19}$$

$$\theta = s^2 [4\delta (h_0 \cos \phi - 4\delta \sin^2 \phi) T_1 - (4h_0^4 \varepsilon \sin \phi + 16h_0^3 \varepsilon \delta \sin \phi \cos \phi) T_2] \tag{20}$$

where the functions appearing satisfy the following differential equations:

$$f_0''' + f_0 f_0'' = 0, \quad f_0(0) = f'_0(0) = f'_0(\infty) - 1 = 0$$

$$\frac{\theta''_{10}}{Pr} + f_0 \theta'_{10} = 0, \quad \theta_{10}(0) = \theta_{10}(\infty) = 0$$

$$L_1 f_i = S_i, \quad f_i(0) = f'_i(0) = f'_i(\infty) = 0, \quad i = 1, 2$$

$$L_1 = (\quad)''' + f_0 (\quad)'' - 2f'_0 (\quad)$$

$$S_1 = f_0'^2 - 1, \quad S_2 = -\theta_{10}$$

$$L_2 F_i = Q_i, \quad F_i(0) = F_i'(0) = F_i'(\infty) = 0, \quad i = 1, 2$$

$$L_2 = (\quad)''' + f_0(\quad)'' - 4f_0'(\quad)' + 5f_0''(\quad)$$

$$Q_1 = -f_0''f_1, \quad Q_2 = -f_0''f_2$$

$$L_3 T_i = R_i, \quad T_i(0) = T_i(\infty) = 0, \quad i = 1, 2$$

$$L_3 = (\quad)''/Pr + f_0(\quad)' - 4f_0'(\quad)$$

$$R_i = -(5F_i + f_i)\theta'_{10}, \quad i = 1, 2.$$

It can be observed that, like in classical boundary layer analysis, the normal velocity component in the boundary layer has not been matched with that in the core. This unmatched velocity component gives the boundary condition for the higher order core solution.

In case II, the thermal boundary condition on the wall is of constant flux, that is

$$\frac{\partial T}{\partial R} = q_w \quad \text{on } R = a. \quad (21)$$

Since the length scale in the radial direction in the boundary layer is $Re^{-1/2}$, we now non-dimensionalize temperature as

$$\theta = (T - T_0)k Re^{1/2}/q_w a \quad (22)$$

the other non-dimensional variables being the same as before. The core solution in this case is

$$u^c = v^c = \theta^c = 0, \quad w^c = 1/h, \quad p^c = -1/2h^2.$$

The boundary layer equations along with the boundary and matching conditions in this case suggest expansions in half integer powers of s as

$$Y_1 = \sum_{n=0}^{\infty} s^{n/2} Y_{1n} \quad (23)$$

where Y_1 stands for $u, v, w,$ or θ , and $\theta_1 = \theta/h_0$ in this case. The velocity and temperature in the boundary layer are thus given by

$$u_1 = (f_0 - \eta f_0') + s^2 [4\delta^2 \sin^2 \phi F' + 4\delta(h_0 \cos \phi - \delta \sin^2 \phi)(F + 5G_1 - \eta G_1')] + s^{5/2} [6G_2 - \eta G_2' + 4\epsilon \delta h_0^4 \sin \phi \cos \phi H' - (4\epsilon h_0^5 \sin \phi - 20h_0^4 \epsilon \delta \sin \phi \cos \phi)H] \quad (24)$$

$$v_1 = \frac{2\delta \sin \phi}{h_0} F' s + 2h_0^3 \epsilon \delta \cos \phi H' s^{3/2} \quad (25)$$

$$w_1 = f_0' + s^2 [4\delta(h_0 \cos \phi - \delta \sin^2 \phi)G_1'] - s^{5/2} [(20h_0^4 \epsilon \delta \sin \phi \cos \phi + 4\epsilon h_0^5 \sin \phi)G_2'] \quad (26)$$

$$\theta_1 = s^{1/2} \theta_{11} + [4\delta(h_0 \cos \phi - \delta \sin^2 \phi)P_1 + 4\delta^2 \sin^2 \phi P_2 + 4h_0^2 \delta^2 \sin^2 \phi P_3] s^{5/2} + [-(4\epsilon h_0^5 \sin \phi + 20\delta \epsilon h_0^4 \sin \phi \cos \phi)T_1 + 4h_0^4 \epsilon \delta \sin \phi \cos \phi T_2 + 4\epsilon \delta h_0^6 \sin \phi \cos \phi T_3] s^3 \quad (27)$$

where the functions occurring satisfy the following differential equations:

$$f_0''' + f_0 f_0'' = 0, \quad f_0(0) = f_0'(0) = f_0'(\infty) - 1 = 0$$

$$\frac{\theta_{11}''}{Pr} + f_0 \theta_{11}' - f_0' \theta_{11} = 0, \quad \theta_{11}(0) + \sqrt{2} = \theta_{11}(\infty) = 0$$

$$F''' + f_0 F'' - 2f_0' F' = f_0'^2 - 1,$$

$$F(0) = F'(0) = F'(\infty) = 0$$

$$H''' + f_0 H'' - 3f_0' H' = -\theta_{11},$$

$$H(0) = H'(0) = H'(\infty) = 0$$

$$G_1''' + f_0 G_1'' - 4f_0' G_1' + 5f_0'' G_1 = -F' f_0'',$$

$$G_1(0) = G_1'(0) = G_1'(\infty) = 0$$

$$G_2''' + f_0 G_2'' - 5f_0' G_2' + 6f_0'' G_2 = -H f_0',$$

$$G_2(0) = G_2'(0) = G_2'(\infty) = 0$$

$$DP_i = Q_i, \quad P_i'(0) = P_i'(\infty) = 0, \quad i = 1, 2, 3$$

where

$$D = \frac{(\quad)''}{Pr} + f_0(\quad)' - 5f_0'(\quad)$$

$$Q_1 = 5G_1 \theta_{11}' - F \theta_{11}$$

$$Q_2 = -F' \theta_{11}$$

$$Q_3 = -F' \theta_{11} + F' \theta_{11}$$

$$L_4 T_i = S_i, \quad T_i(0) = T_i(\infty) = 0, \quad i = 1, 2, 3$$

where

$$L_4 = \frac{(\quad)''}{Pr} + f_0(\quad)' - 6f_0'(\quad)$$

$$S_1 = -6G_2 \theta_{11}' - H \theta_{11}' + G_2' \theta_{11}$$

$$S_2 = -H' \theta_{11}$$

$$S_3 = H' \theta_{11}' - H' \theta_{11}$$

RESULTS AND DISCUSSIONS

In this paper, we have studied the flow development in a heated curved pipe. Two different kinds of heating—a constant temperature T_w at the wall, and a constant flux of heat q_w at the wall have been considered. Before going into the results, we will give a brief description of the physics of the flow.

To begin with, suppose that the flow is taking place in an unheated curved pipe. Because of curvature, a pressure gradient is set up towards the centre of curvature to balance the centrifugal force arising out of curvature. This pressure gradient varies across the cross-section, and thus sets up a secondary motion symmetric about the central plane. This secondary flow is superimposed on the primary motion, and has been discussed by Singh [11] and Pedley [13]. When heat is added to the system, a second secondary motion arising out of the buoyancy effect is also super-

imposed on the primary flow. Yao [10] has considered the entry flow in a heated straight pipe, and has established the existence of this secondary motion.

The equation governing the various functions occurring in the velocity and temperature fields are nonlinear and coupled, and hence no analytical solution is possible. We have therefore solved them numerically, adopting the Runge–Kutta–Gill method with the shooting technique.

The nondimensionalization, as well as the perturbation scheme have been introduced with a view to avoid the restriction on the curvature parameter δ . In equation (10) introduction of the θ dependence through h_0 in w_1 and η incorporates the fact that the axial core velocity is more on the outer bend, and that the boundary layer thickness is less there. This means, to leading order the flow is the same as the Blasius boundary layer flow over a flat plate. The perturbation with respect to the axial coordinate s , is natural when we are looking only at the entry region. Yao [10] has perturbed with respect to ε and hence had to restrict the analysis to small values of ε . In our analysis, we have overcome this restriction on ε and δ .

In case I, the axial velocity in the boundary layer is

given by equation (19). The first term of $O(1)$ represents the Blasius boundary layer velocity. This is because, the fluid particles have to travel some distance before getting the effect of curvature and heating. These effects are felt at $O(s^2)$. The first term in brackets in equation (19) is due to curvature. Figure 2 depicts the variations of F_1' and F_2' which gives the heating effects on the axial velocity. The latter depends on Prandtl number Pr .

The secondary velocity which is developed has again two components—one due to curvature and another one due to thermal boundary conditions, as can be seen from equations (18) and (25). However, in case I, both the effects are felt at $O(s)$, while in case II, the thermal effect is felt only at $O(s^{3/2})$. To start with, the flow does not have any azimuthal velocity, but curvature and heating introduces the secondary flow. These effects have been observed by Pedley [13] for flow in an unheated curved pipe, and by Yao [10] in a straight heated pipe. Figures 3 and 4 depict the secondary velocity at various cross-sections. In case I, it is positive at the outer bend, and negative at the inner bend, while in case II, it is vice versa. This suggests that the secondary flow developed is different

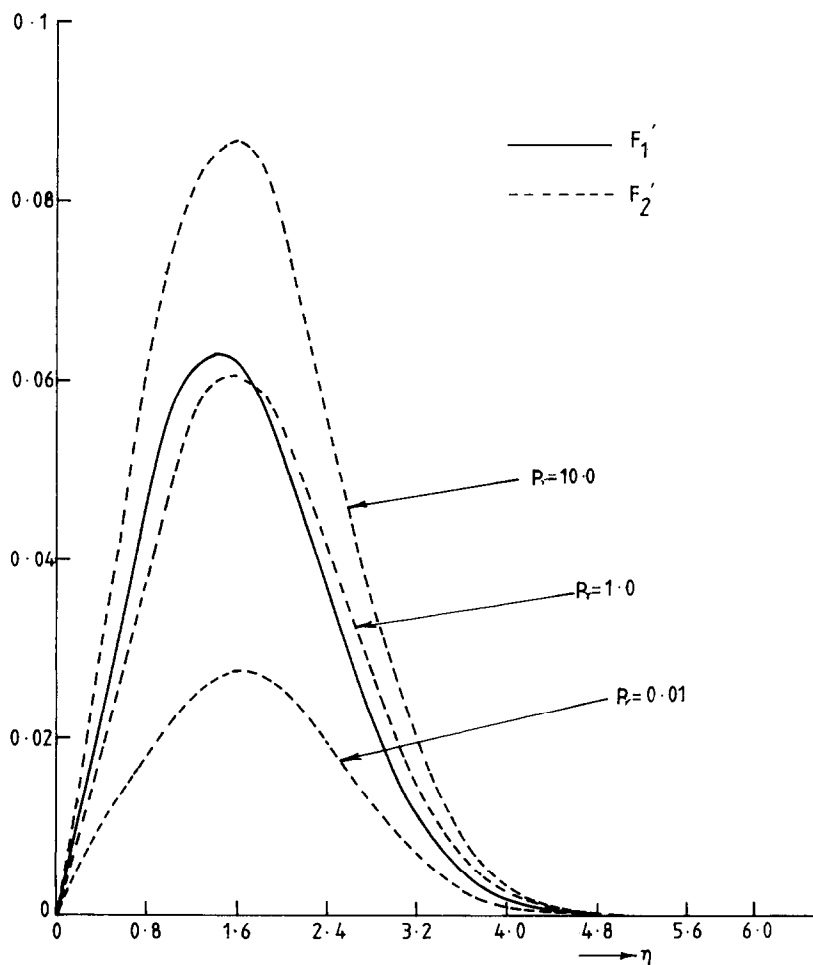


FIG. 2. Effects of curvature and heating on axial velocity in the boundary layer—case I.

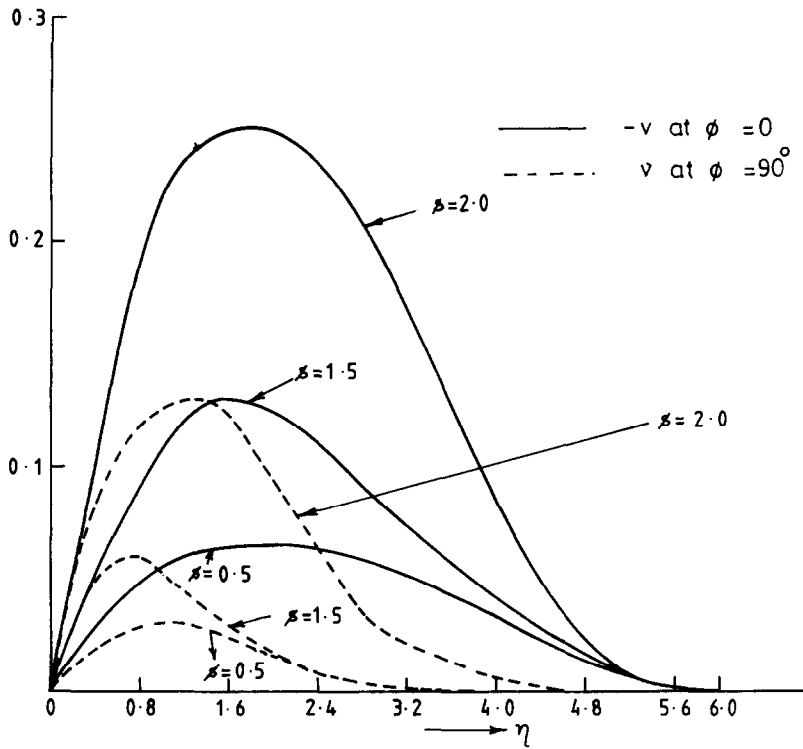


FIG. 3. Secondary velocity in the boundary layer—case I.

in the two cases. It can also be seen from the figures, that the secondary velocity grows as we go downstream, and we can expect that when the flow is fully developed, the secondary flow will tend to that obtained by Yao and Berger [14].

Figures 5 and 6 represent the temperature distribution in the boundary layer in the two cases. It can be observed that though the wall is maintained at constant temperature both axially and azimuthally, the boundary layer heating is not uniform. It gets

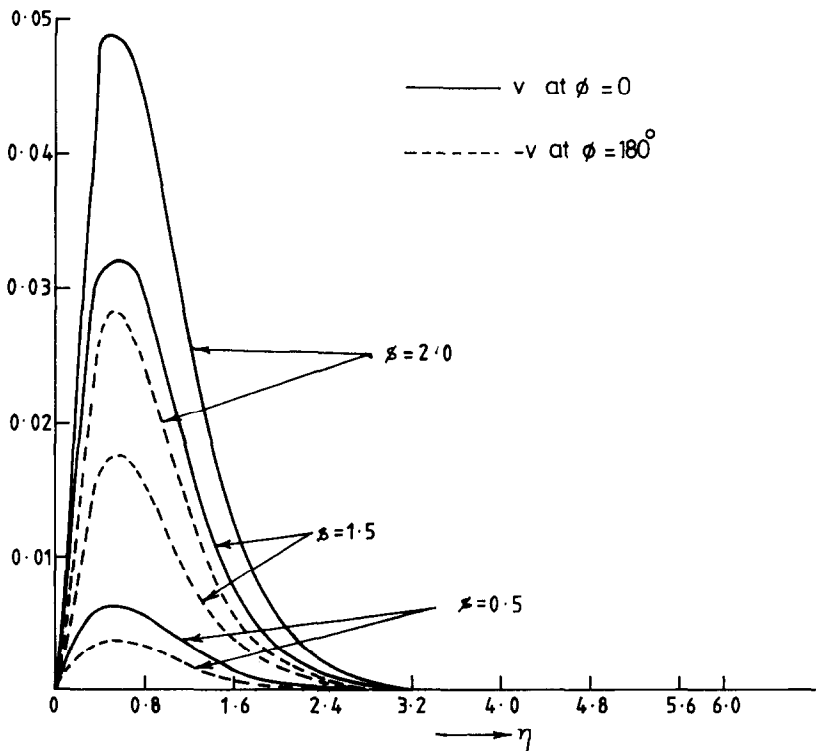


FIG. 4. Secondary velocity in the boundary layer—case II.

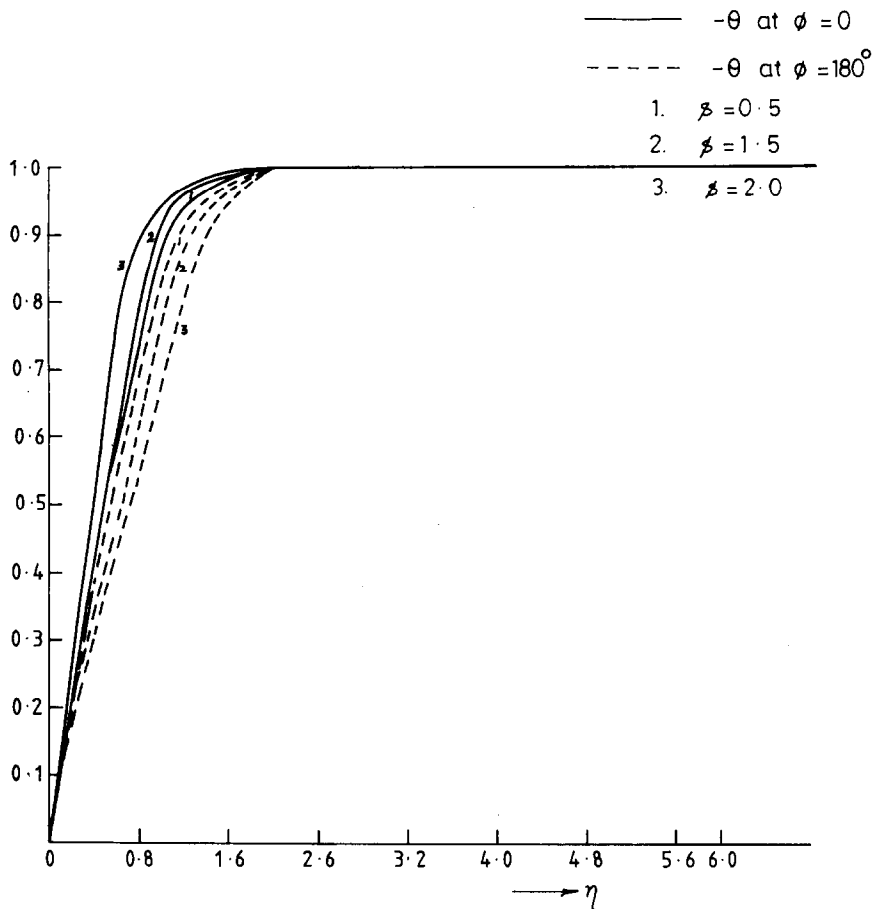


FIG. 5. Temperature distribution in the boundary layer at inner and outer bends—case I.

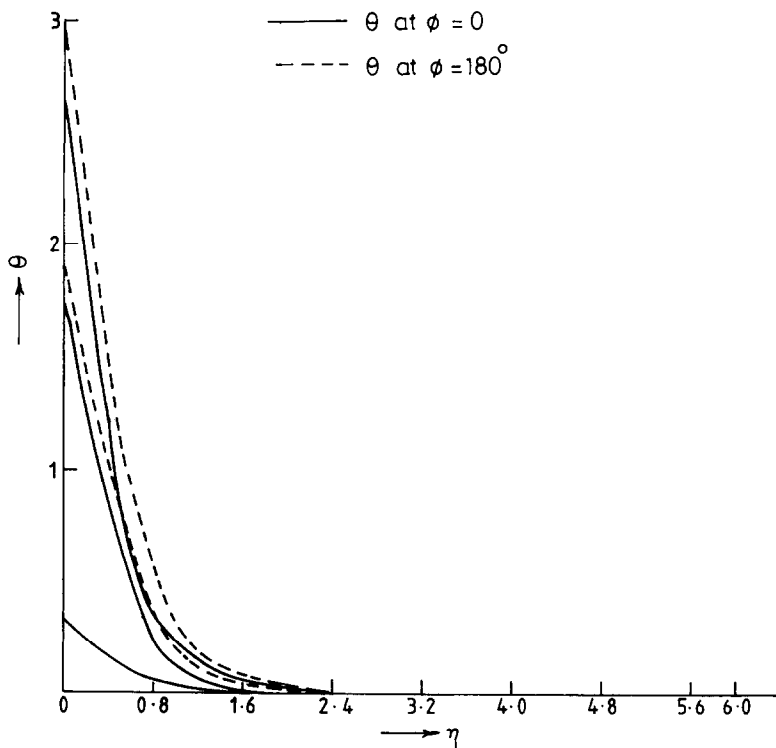


FIG. 6. Temperature distribution in the boundary layer at inner and outer bends—case II.

heated up more on the inner bend than at the outer bend. The same observation can be made in the second case as well, even though there is a constant flux of heat throughout. A possible reason for this could be that the fluid particles near the outer bend, before getting heated, are swept to the inside bend by the secondary velocity.

The non-dimensional shear stresses are given by

$$T_{rz} = -\frac{\beta}{h_0^2\sqrt{(2s)}} w_{1\eta}$$

$$T_{r\phi} = -\frac{\beta}{h_0\sqrt{(2s)}} v_{1\eta}$$

and hence are in the two cases given by

$$T_r^I = -\frac{\beta}{h_0\sqrt{(2s)}} [f_0''(0) + s^2 \{4\delta(h_0 \cos \phi - \delta \sin^2 \phi) F_1''(0) + (4h_0^4 \epsilon \sin \phi + 16h_0^3 \epsilon \delta \sin \phi \cos \phi) F_2''(0)\}] \quad (28)$$

$$T_{r\phi}^I = -\frac{\beta s}{h_0\sqrt{(2s)}} \left[\frac{2\delta \sin \phi}{h_0} f_1''(0) + 2h_0^2 \epsilon \cos \phi f_2''(0) \right] \quad (29)$$

$$T_r^{II} = -\frac{\beta}{h_0^2\sqrt{(2s)}} [f_0''(0) + s^2 \cdot 4\delta(h_0 \cos \phi - \delta^2 \sin^2 \phi) G_1''(0) - s^{5/2} (20h_0^4 \epsilon \delta \sin \phi \cos \phi + 4\epsilon h_0^5 \sin \phi) G_2''(0)] \quad (30)$$

$$T_{r\phi}^{II} = -\frac{\beta}{h_0\sqrt{(2s)}} \left[\frac{2\delta \sin \phi}{h_0} F''(0) + 2h_0^3 \epsilon \cos \phi H''(0) s^{3/2} \right] \quad (31)$$

It is clear that T_{rz} varies with both s and ϕ . In the case of an unheated straight pipe, the shearing stress reduces to

$$T_{rz} = -\frac{\beta}{h_0\sqrt{(2s)}} [f_0''(0) + s^2 \cdot 4\delta(h_0 \cos \phi - \delta \sin^2 \phi)]. \quad (32)$$

In such a case, for small s , the stress is a maximum on the inner bend. But as s increases, the point of maximum stress shifts to the outer bend, the shifting taking place at $s = 1.92(1 - \delta^2)^{-1/2}$. However, in the presence of thermal boundary conditions, we cannot obtain such an explicit expression for the changeover. In this case also, initially for small s , the stress is maximum at the inner bend, but as s increases, the $O(s^2)$ terms increase in dominance, and the point of maximum shear shifts to near the outer bend, though it is never at the outer bend. In the case of constant temperature conditions, it is near $\phi = 60^\circ$, and in the case of constant heat flux, it is near $\phi = 330^\circ$. The shear being initially more on the inner bend is because,

for small s , the first term in equations (28) and (30) is dominant, thereby reproducing the features of an entry flow in an unheated pipe. The exact location of the point of maximum shear stress in the two cases are different, and this again suggests that the secondary motion is different in the two cases.

Equations (29) and (31) give the azimuthal shear stress on the wall in the two cases. In case I, we see that the azimuthal shear stress is proportional to axial distance s , and hence motion will be similar in all the cross-sectional planes. To find out the plane about which the secondary motion is symmetrical we find out the point at which the azimuthal shear stress vanishes. It is found from the expressions that in the case of constant temperature input, the azimuthal angle at which $T_{r\phi}$ vanishes is independent of the cross-section, and is given by

$$\phi = \tan^{-1} \left[-\frac{h_0^3 \epsilon}{\delta} \frac{f_{12}''(0)}{f_{11}''(0)} \right].$$

We can obtain the particular cases for an unheated curved pipe and a heated straight pipe from this expression. Thus, in the absence of heating, the azimuthal shear stress vanishes at $\phi = 0^\circ$ and 180° , that is at the outer bend and the inner bend, respectively, as found by Pedley [13], while in the case of a heated straight pipe, it vanishes at $\phi = \pm 90^\circ$, as found by Yao [10]. In the case of a heated curved pipe, the point of vanishing of the azimuthal shear stress depends on the Prandtl number.

In case II, the azimuthal angle at which the azimuthal shear stress vanishes is given by

$$\phi = \tan^{-1} \left[-\frac{h_0^4 \epsilon}{\delta} \frac{H''(0)}{F''(0)} s^{1/2} \right].$$

It is thus a function of the axial distance, and hence the secondary motion depends on the cross-section considered. Thus, we can conclude that the combined effect of buoyancy and curvature is to displace the symmetric nature of the secondary motion, and this displacement depends on the type of thermal input given at the wall.

For the case of flow with constant temperature at the wall, we calculate the heat flux through the Nusselt number, Nu , which is given by

$$Nu = -\frac{2}{\beta h_0\sqrt{(2s)}} [\theta'_{10}(0) + \{4\delta(h_0 \cos \phi - \delta \sin^2 \phi) T_1'(0) - (4h_0^4 \epsilon \sin \phi + 16h_0^3 \epsilon \delta \sin \phi \cos \phi) T_2'(0)\} s^2]. \quad (33)$$

This is depicted in Fig. 7 as a function of ϕ . We see that very near the entrance, at $s = 0.1$, Nu is maximum at the inner bend. However, as we go downstream, the point of maximum Nu shifts towards the outer bend. The explanation is very similar to that for the axial shear stress, for the two expressions are similar. This shift of the point of maximum Nu to near the outer bend is more pronounced at $Pr = 10$. As Pr is

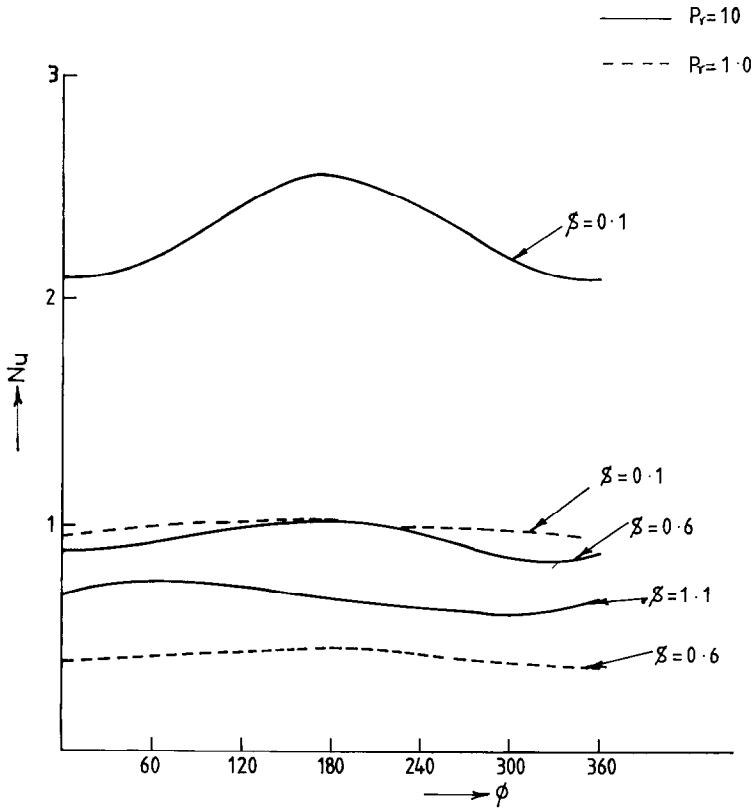


FIG. 7. Variation of Nusselt number with azimuthal angle—case I.

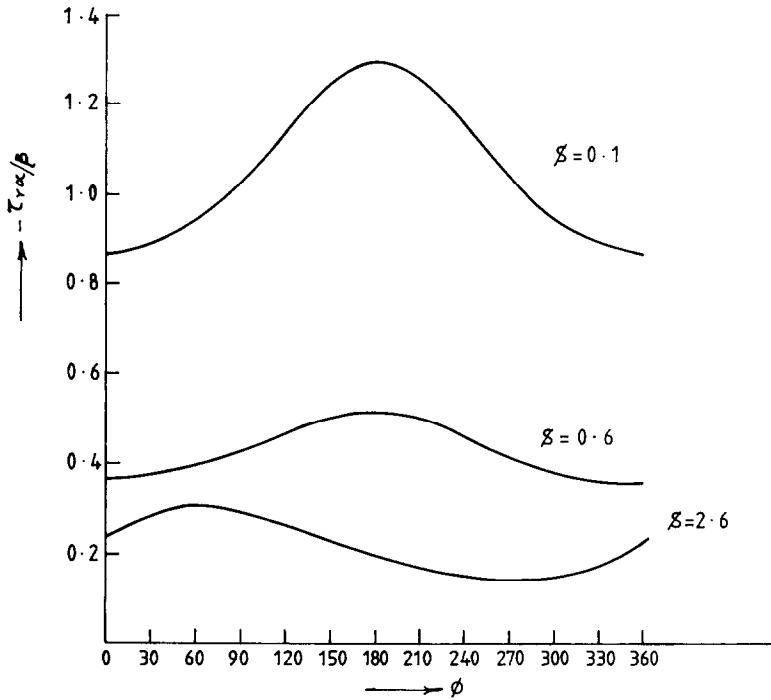


FIG. 8. Variation of axial shear stress with azimuthal angle—cases I and II.

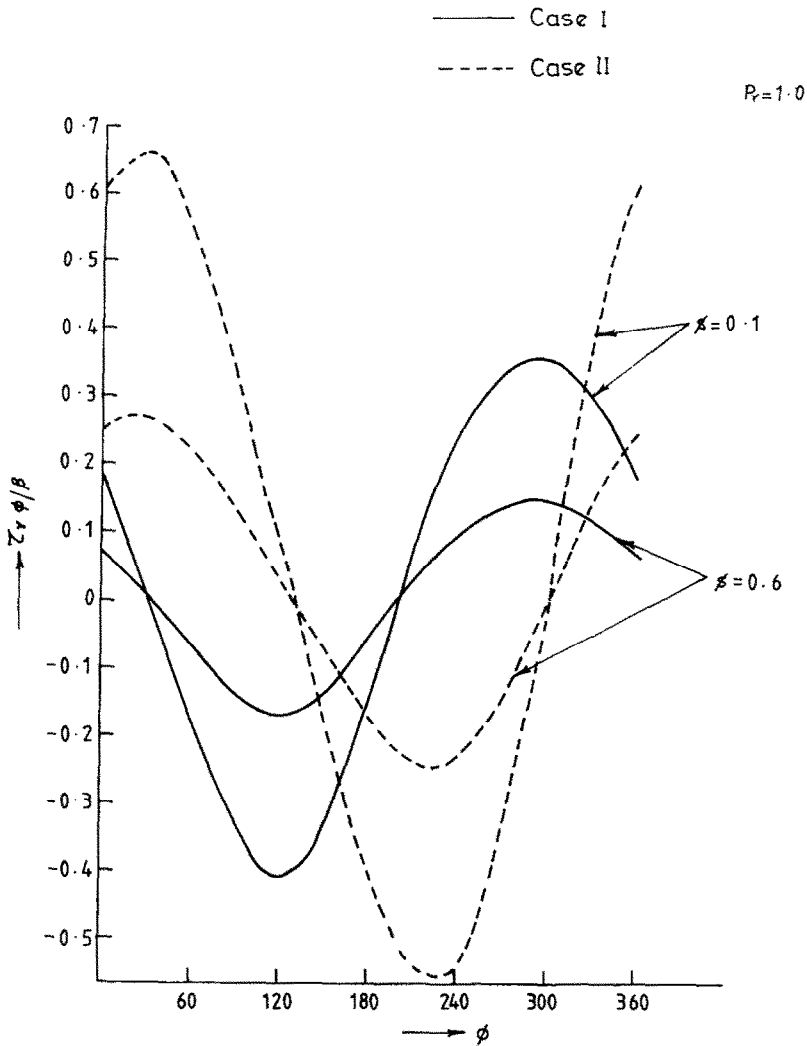


FIG. 9. Variation of azimuthal shear stress with azimuthal angle.

increased, the oscillatory nature of Nu is not so evident. The variations of the shear stress are plotted in Figs. 8 and 9.

It should be noted that in obtaining the boundary conditions for the boundary layer velocity components, the matching has been done only for the axial and azimuthal velocity components. The radial velocity component in the boundary layer has not been matched. This is true in any boundary layer analysis, and gives rise to the displacement effect in the core. In view of the s -perturbation used in this study to avoid the restriction on δ , the displacement effect on the core cannot be analysed. This aspect has been studied in a companion paper under preparation.

REFERENCES

1. B. R. Morton, Laminar convection in uniformly heated horizontal pipes at low Rayleigh numbers, *Q. J. Mech. Appl. Math.* **12**, 410-420 (1969).
2. Y. Mori and W. Nakayama, Forced convective heat transfer in a straight pipe rotating around a parallel axis, *Int. J. Heat Mass Transfer* **10**, 1179-1194 (1967).
3. C. V. Mahalakshmi and R. Devanathan, Laminar forced free convection in horizontal tubes of varying cross-sections at low Rayleigh number, *Ind. J. Pure Appl. Math.* **13**, 946-958 (1982).
4. W. R. Dean, A note on the motion of a fluid in a curved pipe, *Phil. Mag.* **4**, 208-223 (1927).
5. W. R. Dean, The streamline motion of a fluid in a curved pipe, *Phil. Mag.* **5**, 673-695 (1928).
6. D. J. McConologue and R. S. Srivastava, Motion of fluid in a curved tube, *Proc. R. Soc.* **307A**, 37-53 (1968).
7. W. M. Collins and S. C. R. Dennis, The steady motion of a viscous fluid in a curved tube, *Q. J. Mech. Appl. Math.* **28**, 133-156 (1975).
8. S. N. Barua, On secondary flow in stationary curved pipes, *Q. J. Mech. Appl. Math.* **16**, 61-77 (1969).
9. W. T. Lawrence and J. C. Chato, Heat transfer effects on the developing laminar flow inside vertical tubes, *Trans. Am. Soc. Mech. Engrs, Series C, J. Heat Transfer* 214-222 (1966).
10. L. S. Yao, Entry flow in a heated straight tube, *J. Fluid Mech.* **88**, 465-483 (1978).

11. M. P. Singh, Entry flow in a curved pipe, *J. Fluid Mech.* **65**, 517–539 (1974).
12. L. S. Yao and S. A. Berger, Entry flow in a curved pipe, *J. Fluid Mech.* **67**, 177–196 (1975).
13. T. J. Pedley, *The Fluid Mechanics of Large Blood Vessels*. Cambridge University Press, London (1980).
14. L. S. Yao and S. A. Berger, Flow in heated curved pipes, *J. Fluid Mech.* **88**, 339–359 (1978).

ÉCOULEMENT D'ENTRÉE DANS LES TUBES COURBES ET CHAUFFÉS

Résumé—On analyse l'écoulement dans la région d'entrée des tubes courbes et chauffés. On considère les deux cas de température pariétale uniforme et de flux de chaleur uniforme. A partir des approximations de la couche limite et de la méthode des développements asymptotiques, les effets combinés de courbure, d'entrée et de pesanteur sont considérés. On trouve que la pesanteur perturbe l'écoulement secondaire symétrique induit par la courbure, la déviation dépendant du type d'apport de chaleur à la paroi. On trouve aussi que la nature oscillatoire du nombre de Nusselt, à température uniforme, décroît lorsque le nombre de Péclet augmente.

STRÖMUNG IM EINLAUFGEBIET BEHEIZTER GEKRÜMMTER ROHRE

Zusammenfassung—Es wird die Strömung im Einlaufgebiet beheizter gekrümmter Rohre untersucht. Es wird sowohl der Fall konstanter Wandtemperatur als auch konstanter Wand-Wärmestromdichte betrachtet. Unter Verwendung der Grenzschichtnäherungen und der Methode der angepassten Reihenentwicklungen werden die kombinierten Einflüsse der Krümmung, des Einlaufgebietes und des Auftriebes betrachtet. Es zeigt sich, daß der Auftrieb die durch die Krümmung hervorgerufene symmetrische Sekundärbewegung stört. Die Abweichung ist abhängig von der Art der Wärmeeinbringung an der Wand. Man stellt auch fest, daß die Oszillationen der Nusselt-Zahl im Falle konstanter Wandtemperatur mit zunehmender Peclet-Zahl abnehmen.

ТЕЧЕНИЕ В НАЧАЛЬНОМ УЧАСТКЕ КРИВОЛИНЕЙНОЙ НАГРЕВАЕМОЙ ТРУБЫ

Аннотация—Анализируется течение в начальном участке нагреваемых криволинейных труб. Рассматриваются два случая нагрева—постоянная температура стенки и постоянный тепловой поток на ней. В приближении пограничного слоя методом сращиваемых асимптотических разложений изучаются совместные эффекты, обусловленные кривизной трубы, наличием входного участка и подъемной силой. Найдено, что подъемная сила вносит возмущения в симметричное вторичное течение, вызванное кривизной; его величина зависит от способа подачи тепла к стенке. Обнаружено также, что колебательный характер числа Нуссельта в случае постоянной температуры уменьшается с ростом числа Пекле.